Mineralogical Magazine, February 2003, Vol. 67(1), pp. 113–123

Thermodynamics from first principles: temperature and composition of the Earth's core

D. Alfè[1,2,*], M. J. Gillan[1] and G. D. Price[2]

[1] Department of Physics and Astronomy, University College London, Gower Street, London WC1E 6BT, UK
[2] Department of Earth Sciences, University College London, Gower Street, London WC1E 6BT, UK

ABSTRACT

We summarize the main ideas used to determine the thermodynamic properties of pure systems and binary alloys from first principles calculations. These are based on the *ab initio* calculations of free energies. As an application we present the study of iron and iron alloys under Earth's core conditions. In particular, we report the whole melting curve of iron under these conditions, and we put constraints on the composition of the core. We found that iron melts at 6350±600 K at the pressure corresponding to the boundary between the solid inner core and the liquid outer core (ICB). We show that the core could not have been formed from a binary mixture of Fe with S, Si or O and we propose a ternary or quaternary mixture with 8–10% of S/Si in both liquid and solid and an additional ~8% of oxygen in the liquid. Based on this proposed composition we calculate the shift of melting temperature with respect to the melting temperature of pure Fe of ~–700 K, so that our best estimate for the temperature of the Earth's core at ICB is 5650±600 K.

Keywords: thermodynamics, first principles calculations, Earth's core, iron, inner core boundary (ICB).

Introduction

The increasing popularity of density functional theory (DFT) (Parr and Yang, 1989) in the physical, chemical, and more recently geological and biological communities, is due to its exceptional reliability in reproducing experimental results, giving to DFT-based methods unparalleled predictive power. The success of first-principles calculations is also due to the increasingly wide-spread availability of large computational resources, as well as more and more efficient computer codes. Density functional theory has been used extensively to study the static, zero-temperature properties of materials (Pickett, 1989). Recently, the finite temperature properties of solids based on the harmonic approximation have also become available (Karki *et al.*, 2000; Lichtenstein *et al.*, 2000; Kern *et al.*, 1999; Alfè *et al.*, 2001). The introduction of molecular dynamics in *ab initio* calculations (Car and Parrinello, 1985) extended the range of applicability of first-principles calculations to liquids and non-harmonic solids, with the possibility of accessing the full dynamic and thermodynamic properties of solids and liquids. However, finite-temperature calculations are based on statistical sampling of ensembles, and for their very nature are intrinsically more expensive than static calculations. For this reason, it has only been in the last few years that these techniques have been applied to the systematic study of finite temperature properties. The first work which combined finite temperature thermodynamics of solid and liquid from first principles was that of Sugino and Car (1995), who calculated the free energy of solid and liquid Si using DFT with the local density approximation (LDA) and obtained the zero pressure melting point of silicon. Later de Wijs *et al.* (1998) calculated the zero-pressure melting point of Al and we calculated the whole melting curve of Al in the 0–150 GPa pressure range (Vočadlo and Alfè, 2002).

* E-mail: ucfbdxa@ucl.ac.uk
DOI: 10.1180/0026461026610089

The melting curve of iron under Earth's core conditions, and a study of the chemistry of the Earth's core are the subjects of this paper. Here we summarize the main points of this work; a detailed description of the techniques and the results have been published elsewhere (Alfè *et al.*, 1999*a*, 2000*d*, 2001, 2002*a,b,c*).

The temperature of the Earth's core is one of the major uncertainties in the Earth's sciences. This is a fundamental parameter needed in order to understand the thermal budget and all the dynamic processes of the planet, including volcanism and plate tectonics. As yet there is no direct way of getting to the temperature of the core, and it is unlikely that this situation will change in the future. However, there is an indirect route that has been followed for a number of years: if we assume that the core is pure iron, then at the boundary between the solid and the liquid (ICB) the temperature must be the melting temperature of iron at ICB pressure. So, if we can measure the melting curve of iron up to core pressures we have a close estimate of the temperature of the core. This is by no means an easy task, since the conditions are extreme, at ICB the pressure is 330 GPa and the temperature is several thousands of degrees. At these conditions, the only experiments that are possible at the moment are those based on shock waves (Yoo *et al.*, 1993; Brown and McQueen, 1986). In these experiments it is very difficult to measure the temperature, and in general this is only estimated. At lower pressures, up to ~200 GPa, diamond anvil cell experiments are possible (Boehler, 1993; Saxena *et al.*, 1994; Shen *et al.*, 1998; Errandonea *et al.*, 2001; Williams *et al.*, 1987); however, even at pressures as low as 60 GPa there is no definite consensus on the melting temperature of iron. Recently, several theoretical attempts to calculate the melting curve of iron (Alfè *et al.*, 1999*a*, 2002*a*; Laio *et al.*, 2000; Belonoshko *et al.*, 2000) have been reported.

Here we summarize our own work (Alfè *et al.*, 1999*a*, 2002*a*), and we report the full melting curve of iron from 50 to 350 GPa, calculated using first-principles calculations of free energies. The other two theoretical calculations of the high-pressure melting curve of iron (Laio *et al.*, 2000; Belonoshko *et al.*, 2000) used first principles in a different way. Free energies of liquid and solid were not calculated, but instead, empirically parameterized potentials were fitted to the *ab initio* calculations. The empirical potential was then used to simulate very large systems containing coexisting solid and liquid. We ourselves have followed this route to get to the melting temperature, and we have shown that once appropriate corrections are made, the results are identical to those obtained from the full calculation of free energies (Alfè *et al.*, 2002*c*). No such corrections, however, were made in previous works (Laio *et al.*, 2000; Belonoshko *et al.*, 2000).

The composition of the Earth's core is a second major uncertainty in the Earth's sciences (Birch, 1952; Birch, 1964; Ringwood, 1977; Poirier, 1994). It is generally accepted that the core must contain mainly iron (Birch, 1964). However, the density of the outer liquid core is 6–10% less than that estimated for pure iron (Birch, 1964; Ringwood, 1977; Poirier, 1994), so the outer core must contain a significant amount of light elements. To a lesser extent this is also true for the solid inner core (Jephcoat and Olson, 1987). The leading candidates are S, Si and O (Poirier, 1994), but after decades of discussions there is still no general agreement. The composition of the Earth's core is important for at least two reasons. First, it will help us understand the formation history of the Earth (Ringwood, 1977). Second, as the inner core freezes, light elements are released in the outer core, and it is believed that this generates compositional convection (Loper, 1978), which is ultimately responsible for the generation of the Earth's magnetic field.

The detailed DFT techniques used in this work are identical to those used in our work on hexagonal close packed (h.c.p.) Fe (Alfè *et al.*, 2001). In particular, we use the generalized gradient approximation (GGA) for exchange-correlation energy, in the form known as Perdew-Wang 1991 (Wang and Perdew, 1991), which reproduces very accurately a wide range of experimental properties of solid iron, as noted in more detail elsewhere (Stixrude *et al.*, 1994; Söderlind *et al.*, 1996; Vočadlo *et al.*, 1997; Alfè *et al.*, 2000*b*). We also use the projector-augmented-wave (PAW) implementation of DFT (Blöchl, 1994; Kresse and Joubert, 1999), which is an all-electron technique similar to other standard implementations such as full-potential augmented plane waves (FLAPW) (Wei and Krakauer, 1985), as well as being closely related to the ultrasoft pseudopotential method (Vanderbilt, 1990). We have used the VASP code (Kresse and Furthmüller, 1996), which is exceptionally stable and efficient for metals, with the implementation of an extrapolation of the

charge density which increases the efficiency of molecular dynamics simulations by almost a factor of two (Alfè, 1999*c*).

The paper is organized as follows: in the next section we discuss the calculations of the free energies of liquid and solid iron, and a combination of the two to determine the whole melting curve under Earth's core conditions. In the following section we illustrate the calculations of the free energies of solutes in binary mixtures for both liquid and solid, and how this can be combined to determine the partioning of the solute between the two phases.

The *ab initio* melting curve of iron

At the conditions of the Earth's core the stable solid phase of iron is h.c.p. (Vočadlo *et al.*, 2000), so this is the solid structure considered in our calculations. To determine the melting curve of iron we calculate the chemical potential μ of pure iron as a function of pressure and temperature for both solid and liquid. In a one-component system this is the same as the Gibbs free energy per atom G. In fact, we calculate the Helmholtz free energy F as a function of volume and temperature and then we obtain G from its usual relation $G = F + pV$, where $p = -(\partial F/\partial V)_T$ is the pressure. For any fixed pressure, the continuity of G with respect to temperature defines the melting transition, which is determined by the point where the Gibbs free energies of liquid and solid become equal, $G_l(p,T_m) = G_s(p,T_m)$. The accuracy in the melting temperature, T_m, depends on the relative accuracy in the calculation of G_l and G_s, as the point where they cross will be affected by a relative shift of one curve with respect to the other. Since the difference in the slope of the two free energies is equal to the entropy change on melting, which is, in general, of the order of one Boltzmann constant per atom, one can easily see that for an error of ~100 K in the melting temperature one has to reduce the relative error in G_l and G_s to < ~10 meV/atom. There is no way that DFT can reach this sort of accuracy in the calculation of absolute energies. However, high accuracy is achievable when dealing with energy differences, especially if the solid and the liquid have very similar electronic structure and geometry, as in the case of iron.

In the next two sections we summarize the main ideas used in our calculations of the Helmholtz free energies for liquid and solid.

Free energy of the liquid

The Helmholtz free energy, F, of a classical system containing N particles is:

$$F \supset -k_B T \ln \left\{ \frac{1}{N!\Lambda^{3N}} \int_V d\mathbf{R}_1, ..., d\mathbf{R}_N \; e^{-\beta U(\mathbf{R}_1,...,\mathbf{R}_N;T)/k_B T} \right\} \quad (1)$$

where $\Lambda = h/(2\pi M k_B T)^{1/2}$ is the thermal wavelength, with M the nuclear mass, h the Plank's constant, k_B the Boltzmann constant and $\beta = 1/k_B T$. The multidimensional integral extends over the total volume of the system V. A direct calculation of F using the equation above is impossible, since it would involve knowledge of the potential energy $U(\mathbf{R}_1,..., \mathbf{R}_N;T)$ for all possible positions of the N atoms in the system. We use instead the technique known as "thermodynamic integration" (Frenkel and Smit, 1996), as developed in earlier papers (Sugino and Car, 1995; de Wijs *et al.*, 1998; Alfè *et al.*, 2000*a*). This is a general scheme to compute the free energy difference $F - F_0$ between two systems whose potential energies are U and U_0, respectively. In what follows we will assume that F is the unknown free energy of the *ab initio* system and F_0 the known free energy of a reference system. The free energy difference $F - F_0$ is the reversible work done when the potential energy function U_0 is continuously and reversibly switched to U. To do this switching, a continuous variable energy function U_λ is defined such that for $\lambda = 0$; $U_\lambda = U_0$ and for $\lambda = 1$; $U_\lambda = U$. It is easy to see that the free energy difference in the switching is:

$$\Delta F \supset F - F_0 \supset \int_0^1 d\lambda \left\langle \frac{\partial U}{\partial \lambda} \right\rangle_\lambda \quad (2)$$

For our calculations we define U_λ thus:

$$U_\lambda = (1 - \lambda)U_0 + \lambda U_1 \quad (3)$$

Differentiating U_λ with respect to λ and substituting into equation 2 above yields:

$$\Delta F \supset \int_0^1 d\lambda \langle U - U_0 \rangle_\lambda \quad (4)$$

We calculate the thermal average $\langle \cdot \rangle_\lambda$ using *ab initio* molecular dynamics and averaging over time, with the evolution of the system determined by the potential energy function U_λ.

It is clear from equation 2 that the final result does not depend on the choice of the reference system, but the efficiency of the calculations does. This is because in the evaluation of the thermal average $\langle U - U_0 \rangle_\lambda$ with a chosen accuracy, the strength of the fluctuations of the difference $U - U_0$ determines the length of the simulation. It is absolutely crucial to find a reference system in such a way that the fluctuations in $U - U_0$ are as small as possible. This also minimizes the dependence of $\langle U - U_0 \rangle_\lambda$ on λ, so that a small number of points are needed to compute the integral in equation 2.

We experimented with a number of classical potentials as possible candidates, and we found that an exceptionally good reference system is a simple sum of inverse power potentials:

$$U_{\mathrm{IP}} \supset \frac{1}{2}\sum_{i \not= j} \phi(|\mathbf{R}_i - \mathbf{R}_j|) \qquad (5)$$

where

$$\phi(r) \supset \frac{B}{r^\alpha} \qquad (6)$$

with the parameters B and α chosen so as to minimize the fluctuations in the energy differences between the *ab initio* and the classical systems.

The free energy of the inverse power potential was calculated using thermodynamic integration, with the Lennard-Jones potential as a reference system. The free energy of the Lennard-Jones system has been studied in detail in the past and has been tabulated as a function of density and temperature (Johnson *et al.*, 1993). To be free from possible errors in the reported free energy of the Lennard-Jones we have also repeated most of the calculations starting with the perfect gas as a reference system, and found only a small (but systematic) difference of ~5 meV/atom.

To calculate the free energy of the *ab initio* system we used cells containing 67 atoms with Γ-point only sampling. We carefully checked that errors due to **k**-point sampling and cell size were under control. We repeated the calculations at a number of thermodynamic states spanning the conditions of the Earth's core and fitted the free energy to polynomial in volume and temperature.

Free energy of the solid

The free energy of the solid can be separated as the sum of three contributions, the first is the perfect non-vibrating h.c.p. crystal, F_{perf} (it is a free energy because of the electronic entropy) and the other two arising from the atomic vibrations:

$$F_{\mathrm{sol}}(V,T) = F_{\mathrm{perf}}(V,T) + F_{\mathrm{harm}}(V,T) + F_{\mathrm{anharm}}(V,T) \qquad (7)$$

where F_{harm} is the free energy of the high temperature crystal in the harmonic approximation and F_{anharm} the anharmonic contribution.

The term $F_{\mathrm{perf}}(V,T)$ is easily calculated on the perfect h.c.p. crystal as a function of volume and electronic temperature. These are quick calculations and can be performed on a small workstation.

The free energy of the harmonic crystal is shown in equation 8 below. We truncate the summation after the first term which is the classical contribution of the phonons to the free energy:

$$F_{\mathrm{harm}} \supset -\left(\frac{3k_{\mathrm{B}}T}{\Omega_{\mathrm{BZ}}N_i}\right)\sum_i \int_{\mathrm{BZ}} \left(\ln\left[\frac{k_{\mathrm{B}}T}{\hbar\omega_{\mathbf{q},i}}\right]\right) \mathrm{d}\mathbf{q} \qquad (9)$$

We take the classical limit of the free energy of the harmonic crystal to be consistent with our calculations for the liquid. In any case, the quantum corrections at temperatures above 4000 K are <1 meV/atom.

To calculate the vibrational frequencies, $\omega_{\mathbf{q},i}$, we used our own implementation (Alfè, 1998) of the small displacement method (Kresse *et al.*, 1995). We repeated the calculations at a number of thermodynamic states and fitted the results with polynomials in V and T.

The anharmonic contribution F_{anharm} is calculated again using thermodynamic integration,

$$F_{\mathrm{harm}}(V,T) \supset -\left(\frac{3k_{\mathrm{B}}T}{\Omega_{\mathrm{BZ}}N_i}\right)\sum_i \int_{\mathrm{BZ}} \left(\ln\left[\frac{k_{\mathrm{B}}T}{\hbar\omega_{\mathbf{q},i}(V,T)}\right] - \frac{1}{24}\left[\frac{\hbar\omega_{\mathrm{q},i}(V,T)}{k_{\mathrm{B}}T}\right] + \cdots\right) \mathrm{d}\mathbf{q} \qquad (8)$$

$\omega_{\mathrm{q},i}(V,T)$ are the phonon frequencies of branch i and wavevector $\mathbf{q}$, Ω_{BZ} is the volume of the Brillouin zone, N_i is the

where we chose to use as a reference system a linear combination of the *ab initio* harmonic potential and the inverse power used in the calculations for the liquid. It is easy to show that the leading term in the anharmonic contribution to the free energy is quadratic in the temperature. In fact, we found that F_{anharm} could be well described by the form $a(V)T^2$.

The melting curve

In Fig. 1 we report our melting curve as a continuous line together with some experimental data. Our calculated melting temperature at the ICB pressure of 330 GPa is 6350 K. This is ~300 K lower than previously reported (Alfè *et al.*, 1999*a*), and this lowering is the result of an extensive refinement of our calculations for the free energy of the solid. In the low-pressure region the data come from diamond anvil cell (DAC) experiments. Our results fall ~1000 K above the data from Boehler (1993) and ~500 K above more recent experiments (Shen *et al.*, 1998). In the high-pressure region, only shock wave data are available (Yoo *et al.*, 1993; Brown and McQueen, 1986), for which only the pressure can be measured with a sufficient degree of accuracy. The temperature is not measured directly, but it is calculated using a thermodynamic expression involving the Grüneisen parameter and the specific heat, for which some assumptions must be made.

We want to touch on an important point here, which is related to the quality of the *ab initio* calculations themselves. As we already mentioned previously, we certainly do not expect high accuracy in the absolute calculations of the free energy of liquid and solid, but we do expect large cancellation of errors between liquid and solid, so that the DFT error on the melting curve should not be large. However, there is one clear systematic error in the description of h.c.p. iron with DFT-GGA, and this is the slight underestimation of the pressure, by ~8 GPa in the high-pressure region (ICB conditions) and somewhat more in the low-pressure region. This error cannot be ascribed to the use of PAW or to pseudopotentials since it also arises in all electron calculations (Stixrude *et al.*, 1994; Söderlind *et al.*, 1996), so it is probably due to the GGA. We assume now that the same error will also be present in the liquid, and see how this error propagates in the melting curve. To do that, we correct the free energy by adding a term to put the pressure right:

$$F' = F - \delta pV \tag{10}$$

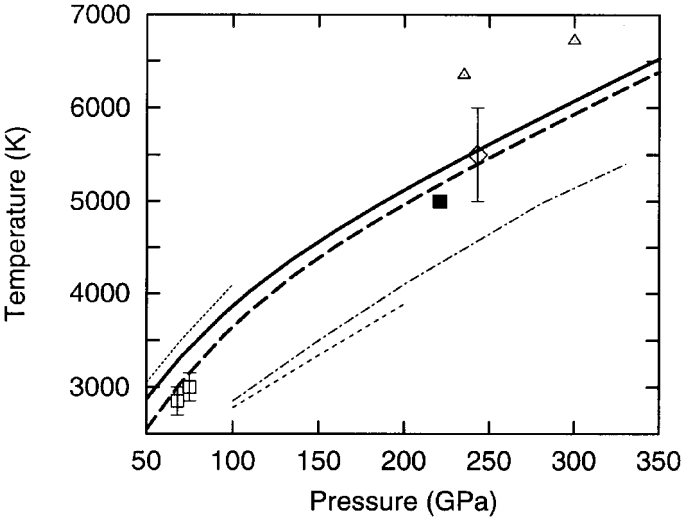

FIG. 1. Comparison of melting curve of Fe from present calculations with previous experimental and *ab initio* results. Heavy solid and dashed curves: present work without and with free-energy correction (see text); chain curve: *ab initio* results of Laio *et al*. (2000); dots, light dashes and squares: DAC measurements of Williams *et al*. (1987), Boehler (1993) and Shen *et al*. (1998); triangles, diamond and solid square: shock experiments of Yoo *et al*. (1993), Brown and McQueen (1986) and Nguyen and Holmes (unpublished). Error bars are those quoted in the original references.

where δp is a volume-dependent correction to the pressure calculated from a fit to the experimental data. We now use the "corrected" free energy F' to calculate the melting curve and report it in Fig. 1 as a dashed line. The effect of the correction is to reduce the melting temperature, and more so in the low-pressure end. The low end of the corrected melting curve is now going through the error bars of the measurements by Shen *et al.* (1998).

Constraints on the composition of the Earth's core

We now turn to the second main aim of this paper: the calculation of the chemical potential of a solute in a solution. As an illustration we use the method to put new constraints on the composition of the Earth's core. The new constraints are based on the following argument. We begin with a working hypothesis: the core is a binary mixture of iron and one light element Fe/*X*. To test this hypothesis we exploit the boundary between the inner and the outer core (ICB). Thermodynamic equilibrium between solid and liquid implies that the chemical potentials of all the constituents have to be equal in the two phases. By calculating the chemical potentials of the impurity *X* in both liquid and solid as a function of concentration and imposing the continuity at ICB we can calculate the partition of the impurity between liquid and solid. Combining this with the density of pure iron we can work out the density jump at ICB. If the calculated density jump is incompatible with the seismological measurements (Masters and Shearer, 1990) the hypothesis will be ruled out. The *ab initio* technical details are exactly the same as for the work on pure iron, but we use ultrasoft pseudopotentials rather than the PAW method.

Chemical equilibrium

The chemical equilibrium between two different phases is characterized by the continuity of the chemical potentials of all species across the phase boundaries. In particular, in the case of a two-species mixture of a solvent *A* and a solute *X* in equilibrium between solid and liquid we have:

$$\mu_X^{\mathrm{l}}(p,T_m,c_X^{\mathrm{l}}) = \mu_X^{\mathrm{s}}(p,T_m,c_X^{\mathrm{s}}) \qquad (11)$$

$$\mu_A^{\mathrm{l}}(p,T_m,c_A^{\mathrm{l}}) = \mu_A^{\mathrm{s}}(p,T_m,c_A^{\mathrm{s}}) \qquad (12)$$

where μ is the chemical potential, p is the pressure, T_m is the melting temperature, c_X is the concentration of solute, and we have used superscripts l and s for liquid and solid, respectively. In the limit of the concentration of the solute c_X going to zero the chemical potential μ_X diverges logarithmically. It is useful then to write

$$\mu_X(p,T_m,c_X) = k_B T \ln c_X + \tilde{\mu}_X(p,T_m,c_X) \qquad (13)$$

so that $\tilde{\mu}_X(p,T_m,c_X)$ is a well behaved quantity for all values of c_X. In ideal solution theory the quantity μ_X is simply assumed to be independent of concentration, but in reality the interaction between solute atoms causes it to vary with c_X. Combining equations 11 and 13 we obtain:

$$c_X^{\mathrm{s}}/c_X^{\mathrm{l}} = \exp[(\mu_X^{\mathrm{l}} - \mu_X^{\mathrm{s}})/k_B T] \qquad (14)$$

This means that the ratio of the mole fractions c_X^{s} and c_X^{l} of *X* in solid and liquid is determined by the thermodynamic quantities μ_X^{l} and μ_X^{s}. The partition of the solute between solid and liquid modifies the melting temperature of the mixture with respect to the melting temperature of pure solvent; it is easy to show that the shift in melting temperature is given by:

$$T_m - T_m^0 \supset \frac{k_B T}{\Delta S_0}(c_X^{\mathrm{s}} - c_X^{\mathrm{l}}) \qquad (15)$$

where T_m^0 is the melting temperature of pure *A* and $\Delta S_0 = S_0^{\mathrm{l}} - S_0^{\mathrm{s}}$ is the entropy change on melting for pure *A*.

We now briefly describe how we calculate the thermodynamic quantities $\tilde{\mu}_X^{\mathrm{s}}$ and $\tilde{\mu}_X^{\mathrm{l}}$ using *ab initio* techniques. A more detailed description of the techniques involved has been reported elsewhere (Alfè *et al.*, 2000*c,d*, 2002*b,d*). The chemical potential of a solute *X* in solid or liquid solvent *A* is equal to the change of Gibbs free energy as one atom of *X* is added to the system at constant pressure p and constant temperature T. Alternatively, it is also equal to the change of Helmholtz free energy as the atom of solute is added at constant volume V and temperature. However, it is impratical to add solute atoms to a system in an *ab initio* simulation. Computationally, it is more convenient to convert solvent into solute, which means working with the difference $\mu_X - \mu_A$ of the chemical potentials of *X* and *A*. The chemical potential μ_X and hence $\tilde{\mu}_X$ is obtained from $\mu_X - \mu_A$ by making use of the Gibbs free energies of pure solid and liquid *A* calculated separately.

Chemical potential in the liquid

To calculate the chemical potential difference $\mu_X - \mu_A$ in the liquid we make use of thermodynamic integration. In the limit of zero concentration this is just the change of Helmholtz free energy as one atom of A is transmuted into X:

$$\Delta F \supset \int_0^1 \mathrm{d}\lambda \langle U_{AX} - U_A \rangle_\lambda \qquad (16)$$

where U_A is the *ab initio* potential energy function for the pure A system and U_{AX} that for the system where one of the A atoms has been converted into X. These calculations demand an unusual kind of simulation. We perform two simultaneous simulations, in the first the system is pure A, and in the second, one of the A atoms has been substituted by an X atom. The positions of all the atoms are the same in the two simulations. We calculate the *ab initio* (free) energies and the forces in both simulations, we move the atoms with the forces $\mathbf{f}_\lambda = \lambda \mathbf{f}_{AX} + (1 - \lambda)\mathbf{f}_A$, where $\mathbf{f}_A$ and $\mathbf{f}_{AX}$ are the forces in the pure A and the A/X systems respectively, and we accumulate the time average of $U_{AX} - U_A$. The simulations are repeated at a sufficient number of λ values so that the integral in equation 16 can be calculated with the required accuracy. To calculate the chemical potential of the solute X away from the dilute limit we repeat the procedure at a finite concentration of X in A, and transmute again one of the A atoms into X. In fact, transmuting only one atom is statistically very inefficient, so we transmute several. This provides an integral of the chemical potential over a range of concentrations, but by repeating the calculations with a different total number of A atoms transmuted into X, the results can be processed to extract the required dependence of the chemical potential on concentration. We found that for small concentrations (<0.2) the chemical potential μ_X can be approximated well by the linear form $\mu_X \approx \mu_X^\dagger + \lambda_X c_X$, where λ_X is a constant (do not confuse λ_X with the dummy parameter λ used in thermodynamic integration).

Chemical potential in the solid

To calculate the chemical potential for the solid we found it convenient to consider the free energy difference between the two systems where one solvent atom A is converted into a solute atom X. It is useful to separate this free energy difference as the sum of three terms:

$$F_X - F_A = F_{XA} = +F_{XA}^{\mathrm{perf}} + F_{XA}^{\mathrm{harm}} + F_{XA}^{\mathrm{anharm}} \qquad (17)$$

where F_{XA}^{perf} is the change of free energy due to substitution of one A atom by an X atom in the perfect non-vibrating crystal, F_{XA}^{harm} is the contribution due to the change in the vibrational frequencies:

$$F_{XA}^{\mathrm{harm}} \supset \frac{3k_B T}{N_s} \sum_s \frac{1}{\Omega_{\mathrm{BZ}}} \int_{\mathrm{BZ}} \mathrm{d}\mathbf{q} \ln \frac{\omega'_{\mathbf{q},s}}{\omega_{\mathbf{q},s}} \qquad (18)$$

Here, N_s is the number of phonon branches (three for each atom in the unit cell), Ω_{BZ} is the volume of the Brillouin zone and $\omega'_{\mathbf{q},s}$, $\omega_{\mathbf{q},s}$ are the phonon frequencies in the A/X and in the pure A systems respectively. The last term F_{XA}^{anharm} is the remainder, which we call the anharmonic contribution. To calculate F_{XA}^{perf} we calculate first F_A^{perf} in an N atoms perfect crystal and then F_{XA}^{perf} on the same system but with one of the A atoms substituted by one X atom, and relaxing the cell until the forces on all the atoms are zero. To evaluate F_{XA}^{harm} we calculate the phonon frequencies in the whole Brillouin zone for both systems using the small displacement method (Alfè, 1998; Kresse *et al.*, 1995). The anharmonic contribution F_{XA}^{anharm} can be calculated using thermodynamic integration, which has been described in detail in our previous paper (Alfè *et al.*, 2000*d*). This procedure gives us the zero concentration limit of the chemical potential difference $\mu_X - \mu_A$. To calculate $\mu_X - \mu_A$ away from the dilute limit, we note that the part of the statistical mechanics associated with the rearrangement of X atoms on lattice sites is rigorously equivalent to a lattice-gas problem, for which we can use standard Monte Carlo methods (Chandler, 1987) to evaluate the free energy. The crucial input from *ab initio* calculations is then the interaction free energy of X atoms when they are on neighbouring sites. This interaction free energy is just the change of F when a pair of X atoms initially on distant sites are placed on nearest-neighbour sites. The change of E in this process is obtained from a straightforward *ab initio* calculation, and the contribution from the entropy change is obtained from an *ab initio* calculation of the lattice vibrational frequencies for the X-X pair on neighbouring sites.

Results and discussion

Results of the calculations are summarized in Table 1, where we report the values of $\mu_X^\dagger$ and λ_X. We start the discussion for the Fe/S binary

TABLE 1. Calculated chemical potentials (eV units) of impurities in the Earth's liquid outer core and solid inner core. Chemical potential $\mu_X = k_B T \ln c_X + \mu_X$ of impurity X is represented at low mole fraction c_X by the linearized form $_X \approx \mu_X^\dagger + \lambda_X c_X$, with superscripts l and s indicating liquid and solid, respectively.

Impurity	$\mu_X^{\dagger l} - \mu_X^{\dagger s}$	λ_X^l	λ_X^s
S	−0.25±0.04	6.2±0.2	6.0±0.2
Si	−0.05±0.02	3.5±0.1	2.8±0.1
O	−2.6±0.2	3.25±1.3	

system. The difference of chemical potential between solid and liquid is $\mu_S^{\dagger l} - \mu_S^{\dagger s} = -0.25$ eV in the limit of zero concentration. Its negative value favours partitioning of S into the liquid, as expected, but its magnitude is smaller than $k_B T$, so that the partitioning is weak. If we were to ignore the dependence on concentration of the chemical potentials, we would get from equation 14 $c_S^s/c_S^l = 0.66$. More importantly, the dependence of the chemical potential on concentration is such that both μ_s^l and μ_X^s increase strongly with increasing mole fraction of S. This is due to an apparent repulsion among the S atoms and is consistent with what we found in our previous work on Fe/S (Alfè and Gillan, 1998). It arises because the S valence states lie at least ~10 eV below the Fermi energy, so that chemical bonding between S atoms is very weak. If two isolated S atoms are brought together, two Fe-S bonds are lost and one Fe-Fe bond is gained. The relative strengths of the Fe-S and Fe-Fe bonds mean that this process is energetically unfavourable. The dependence of μ^s on c^s causes a deviation from the behaviour of ideal mixtures, which is therefore fully taken into account here. The apparent S-S repulsion (departure from ideality) favours equilibration of concentrations between liquid and solid, and therefore at higher concentrations the partitioning between solid and liquid is even smaller. At the sulphur mole fraction $c_S^l = 0.16$ needed to match the density of the liquid outer core we find the solution $c_S^s = 0.14$. The conclusion is that if the outer core were a binary Fe/S mixture, the mole fraction of S in the inner core would have to be ~14%. But this is completely incompatible with seismic measurements, which give an accurate value for the density difference between liquid and solid at the ICB of 4.5±0.5% (Masters and Shearer, 1990). The reason why this is incompatible is that, according to our earlier *ab initio* calculations (Alfè *et al.*, 1999*a*), the density difference between coexisting liquid and solid pure Fe at the ICB pressure is only ~1.8%. Our present calculations show that the volume of the S atom in both solid and liquid is almost identical to that of Fe. This is true to a sufficient accuracy that the fractional change of density in each phase can be calculated simply as $c_S(m_S - m_{Fe})/m_{Fe}$, where m_S and m_{Fe} are the atomic masses of S and Fe. This means that if c_S^l and c_S^s were equal, the density difference between liquid and solid would remain unchanged at 1.8%. The small difference between c_S^l and c_S^s has the effect of increasing the density difference to only 2.7±0.5%, which is still well below the seismic value of 4.5±0.5%. We therefore rule out the binary Fe/S model for core composition.

For Si, the above argument is even stronger, because the chemical potentials in solid and liquid are even more similar, which means that the binary mixture Fe/Si also has to be ruled out as a possible composition of the Earth's core.

For oxygen, the situation is completely different. The difference of chemical potentials in liquid and solid is very large, $\mu_O^{\dagger l} - \mu_O^{\dagger s} = -2.6$ eV, which implies a strong partitioning between liquid and solid. At the oxygen mole fraction $c_O^l = 0.18$ needed to match the density of the liquid core we find $c_O^s \approx 0.003$, which gives a density discontinuity of 7.8±0.2%, markedly larger than the discontinuity at the ICB. Therefore the binary mixture Fe/O is also incompatible with seismological data.

The reason for the very different behaviour of S/Si on one side, and O on the other, is mainly due to the different sizes of these impurities. Sulphur and silicon are almost the same size as iron at core conditions, and this results in an almost perfect arrangement of these elements as substitutional impurities in the h.c.p. iron crystal. This is the main reason why the chemical potentials of these

impurities are so similar in liquid and solid. For oxygen the situation is completely different. The oxygen atoms are significantly smaller than the iron atoms. They are not small enough to fit in the iron crystal as interstitial impurities, but even as substitutional impurity they do not fit very well, since the rigidity of the Fe crystal prevents an efficient arrangment of the Fe atoms around the O. This rigidity is absent in the liquid, and this is the reason for the strong O partition between liquid and solid.

In conclusion, none of the three binary mixtures can account for the composition of the core. However, it can clearly be accounted for with ternary of quaternary mixtures of these three impurities. *Ab initio* calculations on ternary or quaternary mixtures are certainly feasible, but for the moment they are still too demanding. If we assume that different impurities do not affect the respective chemical potentials we can use the results obtained here to construct a model for the composition of the Earth's core. Since oxygen is hardly going into the solid, we need to use sulphur/silicon to reduce the density of solid iron untill it matches the density of the core. We find that we need ~8% of S/Si. This implies that we must have ~10% of S/Si in the liquid, and to match the density of the liquid we need to add ~8% of oxygen. These results are summarized in Table 2. Using these results in conjunction with equation 15 we also find a shift of melting temperature $\Delta T_m = -700 \pm 100$ K with respect to the melting temperature of pure iron.

Conclusions

We have illustrated the techniques for the calculation of chemical potentials in both pure systems and binary mixtures. As an application of the methods we have presented the whole melting curve of iron under Earth's core conditions and put some new constraints on the composition of the core. These developments open a completely new way to *ab initio* calculations, as we have shown that now finite temperature thermodynamic properties can be calculated to the extent of determining complete melting curves. An additional example of our method is the recent calculation of the melting curve of Al in the range 0–150 GPa (Vočadlo and Alfè, 2002). Moreover, it is now possible to study chemical equilibrium of solutions completely from first principles, without the need to resort to simplified approximated descriptions of the atomic interactions using empirical potentials. We have to acknowledge that these calculations would have not been possible without access to powerful computers, which are therefore the fundamental instrument for this type of theoretical research today and in the days to come.

TABLE 2. Estimated molar percentages of sulphur, silicon and oxygen in the solid inner core and liquid outer core obtained by combining *ab initio* calculations and seismic data. S/Si entries refer to total percentages of S and/or Si.

	Solid	Liquid
S/Si	8.5±2.5	10±2.5
O	0.2±0.1	8.0±2.5

Acknowledgements

The work of DA is supported by a Royal Society University Research Fellowship. We thank NERC and EPSRC for allocations of time on the Cray T3E machines at Edinburgh Parallel Computer Centre and Manchester CSAR service, these allocations being provided through the Minerals Physics Consortium (GST/02/1002) and the UK Car-Parrinello Consortium (GR/M01753). Some of the calculations have been performed on an Origin 2000 machine in the HiperSpace Centre at University College London. We gratefully acknowledge discussions with L. Vočadlo.

References

Alfè, D. and Gillan, M.J. (1998) First-principles simulations of liquid Fe-S under Earth's core conditions. *Physical Review B*, **58**, 8248–8256.

Alfè, D. (1998) Program available at http://chianti.geol.ucl.ac.uk/~dario

Alfè, D., Gillan M.J. and Price, G.D. (1999*a*) The melting curve of iron at the pressures of the Earth's core from *ab initio* calculations. *Nature*, **401**, 462–464.

Alfè, D., Price, G.D. and Gillan, M.J. (1999*b*) Oxygen in the Earth's core: a first-principles study. *Physics of the Earth and Planetary Interiors*, **110**, 191–210.

Alfè, D. (1999*c*) Ab initio molecular dynamics, a simple algorithm for charge extrapolation. *Computer Physics Communications*, **118**, 31–33.

Alfè, D., de Wijs, G.A., Kresse, G. and Gillan, M.J. (2000*a*) Recent developments in ab initio thermo-

dynamics. *International Journal of Quantum Chemistry*, **77**, 871–879.

Alfè, D., Kresse, G. and Gillan, M.J. (2000*b*) Structure and dynamics of liquid iron under Earth's core conditions. *Physical Review B*, **61**, 132–142.

Alfè, D., Gillan M.J. and Price, G.D. (2000*c*) Constraints on the composition of the Earth's core from ab initio calculations. *Nature*, **405**, 172–175.

Alfè, D., Gillan M.J. and Price, G.D. (2000*d*) Thermodynamic stability of Fe/O solid solution at inner-core conditions. *Geophysical Research Letters*, **27**, 2417–2420.

Alfè, D., Gillan, M.J. and Price, G.D. (2001) Thermodynamics of hexagonal-close-packed iron under Earth's core conditions. *Physical Review B*, **64**, 045123, 1–16.

Alfè, D., Gillan M.J. and Price, G.D. (2002*a*) Iron under Earth's core conditions: Liquid-state thermodynamics and high-pressure melting curve from ab initio calculations. *Physical Review B*, **65**, 165118, 1–11.

Alfè, D., Gillan M.J. and Price, G.D. (2002*b*) Composition and temperature of the Earth's core constrained by combining ab initio calculations and seismic data. *Earth and Planetary Science Letters*, **195**, 91–98.

Alfè, D., Price, G.D. and Gillan, M.J. (2002*c*) Complementary approaches to the ab initio calculation of melting properties. *Journal of Chemical Physics*, **116**, 6170–6177.

Alfè, D., Price, G.D. and Gillan, M.J. (2002*d*) Ab initio chemical potentials of solid and liquid solutions and the chemistry of the Earth's core. *Journal of Chemical Physics*, **116**, 7127–7136.

Belonoshko, A.B., Ahuja, R. and Johansson, B. (2000) Quasi-Ab Initio Molecular Dynamic Study of Fe Melting. *Physical Review Letters*, **84**, 3638–3641.

Birch, F. (1952) Elasticity and composition of the Earth's interior. *Journal of Geophysical Research*, **57**, 227–286.

Birch, F. (1964) Density and composition of mantle and core. *Journal of Geophysics Research*, **69**, 4377–4388.

Blöchl, P.E. (1994) Projector augmented-wave method. *Physical Review B*, **50**, 17953–17979.

Boehler, R. (1993) Temperatures in the earth's core from melting-point measurements of iron at high static pressures. *Nature*, **363**, 534–536.

Brown, J.M. and McQueen, R.G. (1986) Phase-transitions, Grüneisen-parameter, and elasticity for shocked iron between 77-Gpa and 400-Gpa. *Journal of Geophysical Research*, **91**, 7485–7494.

Car, R. and Parrinello, M. (1985) Unified Approach for Molecular Dynamics and Density-Functional Theory. *Physical Review Letters*, **55**, 2471–2475.

Chandler, D. (1987) *Introduction to Modern Statistical Mechanics*. Oxford University Press, Oxford, UK.

de Wijs, G.A., Kresse, G. and Gillan, M.J. (1998) First-order phase transitions by first-principles free-energy calculations: The melting of Al. *Physical Review B*, **57**, 8223–8234.

Errandonea, D., Schwager, B., Ditz, R., Gessmann, C., Boehler, R. and Ross, M. (2001) Systematics of transition-metal melting. *Physical Review B*, **63**, 132104, 1–4.

Frenkel, D. and Smit, B. (1996) *Understanding Molecular Simulation*, Academic Press, New York.

Jephcoat, A. and Olson, P. (1987) Is the inner core of the Earth pure iron? *Nature,* **325**, 332–335.

Johnson, K., Zollweg, J.A. and Gubbins, E. (1993) The Lennard-Jones equation of state revisited. *Molecular Physics*, **78**, 591–618.

Karki, B.B., Wentzcovitch, R.M., de Gironcoli, S. and Baroni, S. (2000) Ab initio lattice dynamics of $MgSiO_3$ perovskite at high pressure. *Physical Review B*, **62**, 14750–14756.

Kern, G., Kresse, G. and Hafner, J. (1999) Ab initio calculation of the lattice dynamics and phase diagram of boron nitride. *Physical Review B*, **59**, 8551–8559.

Kresse, G., Furthmüller, J. and Hafner, J. (1995) Ab-initio force-constant approach to phonon dispersion relations of diamond and graphite. *Europhysics Letters*, **32**, 729–734.

Kresse, G. and Furthmüller, J. (1996) Efficient iterative schemes for ab initio total-energy calculations using a plane-wave basis set. *Physical Review B*, **54**, 11169–11186.

Kresse, G. and Joubert, D. (1999) From ultrasoft pseudopotentials to the projector augmented-wave method. *Physical Review B*, **59**, 1758–1775.

Laio, A., Bernard, S., Chiarotti, G.L., Scandolo, S. and Tosatti, E. (2000) Physics of iron at Earth's core conditions. *Science*, **287**, 1027–1030.

Lichtenstein, A.I., Jones, R.O., de Gironcoli, S. and Baroni, S. (2000) Anisotropic thermal expansion in silicates: A density functional study of beta-eucryptite and related materials. *Physical Review B*, **62**, 11487–11493.

Loper, D.E. (1978) The gravitationally powered dynamo. *Geophysical Journal of the Royal Astronomical Society*, **54**, 389–404.

Masters, T.G. and Shearer, P.M. (1990) Summary of seismological constraints on the structure of the earth core. *Journal of Geophysical Research*, **95**, 21691–21695.

Parr, R.G. and Yang, W. (1989) *Density-Functional Theory of Atoms and Molecules*. Oxford University Press, Oxford, UK.

Pickett, W.E. (1989) Pseudopotential methods in condensed matter applications. *Computer Physics Reports*, **9**, 115–197.

Poirier, J.-P. (1994) Light elements in the Earth's outer core: a critical review. *Physics of the Earth and Planetary Interiors*, **85**, 319–337.

Ringwood, A.E. (1977) On the composition of the core and implications for the origin of the Earth. *Geochimica et Cosmochimica Acta*, **11**, 111–135.

Saxena, S.K., Shen, G. and Lazor, P. (1994) Temperatures in earths core based on melting and phase-transformation experiments on iron. *Science*, **264**, 405–407.

Shen, G., Mao, H., Hemley, R.J., Duffy, T.S. and Rivers, M.L. (1998) Melting and crystal structure of iron at high pressures and temperatures. *Geophysical Research Letters*, **25**, 373–376.

Söderlind, P., Moriarty, J.A. and Wills, J.M. (1996) First-principles theory of iron up to earth-core pressures: Structural, vibrational and elastic properties. *Physical Review B*, **53**, 14063–14072.

Stixrude, L., Cohen, R.E. and Singh, D.J. (1994) Iron at high pressure: Linearized-augmented-plane-wave computations in the generalized-gradient approximation. *Physical Review B*, **50**, 6442–6445.

Stixrude, L., Wasserman, E. and Cohen, R.E. (1997) Composition and temperature of the Earth's inner core. *Journal of Geophysical Research*, **102**, 24729–24739.

Sugino, O. and Car, R. (1995) Ab initio molecular dynamics study of first-order phase transitions: melting of silicon. *Physical Review Letters*, **74**, 1823–1826.

Vanderbilt, D. (1990) Soft self-consistent pseudopotentials in a generalized eigenvalue formalism. *Physical Review*, **41**, 7892–7895.

Vočadlo, L., de Wijs, G.A., Kresse, G., Gillan, M.J. and Price, G.D. (1997) First-principles calculations on crystalline and liquid iron at Earth's core conditions. *Faraday Discussions*, **106**, 205–217.

Vočadlo, L. and Alfè, D. (2002) Ab initio melting curve of the fcc phase of aluminum. *Physical Review B*, **65**, 214105, 1–12.

Vočadlo, L., Alfè, D., Brodholt, J.P., Price, G.D. and Gillan, M.J. (2000) Ab initio free energy calculations on the polymorphs of iron at core conditions. *Physics of the Earth and Planetary Interiors*, **117**, 123–137.

Wang, Y. and Perdew, J. (1991) Correlation hole of the spin-polarized electron gas, with exact small-wave-vector and high-density scaling. *Physical Review B*, **44**, 13298–13307.

Wei, S.H. and Krakauer, H. (1985) Local-density-functional calculation of the pressure-induced metallization of BaSe and BaTe. *Physical Review Letters*, **55**, 1200–1203.

Williams, Q., Jeanloz, R., Bass, J.D., Svendesen, B. and Ahrens, T.J. (1987) The melting curve of iron to 250 gigapascals – a constraint on the temperature at earths center. *Science,* **286**, 181–182.

Yoo, C.S., Holmes, N.C., Ross, M., Webb, D.J. and Pike, C. (1993) Shock temperatures and melting of iron at Earth core conditions. *Physical Review Letters*, **70**, 3931–3934.

[*Manuscript received 15 October 2001: revised 21 December 2002*]